

# Novel High Dielectric Constant Nanocomposites of Polyaniline Dispersed with $\gamma$ -Fe<sub>2</sub>O<sub>3</sub> Nanoparticles

N. N. Mallikarjuna,<sup>1</sup> S. K. Manohar,<sup>1</sup> P. V. Kulkarni,<sup>2</sup> A. Venkataraman,<sup>3</sup> T. M. Aminabhavi<sup>4</sup>

<sup>1</sup>Alan G. MacDiarmid Laboratories for Technical Innovation, Department of Chemistry, University of Texas at Dallas, Richardson, Texas 75080

<sup>2</sup>Department of Radiology, University of Texas, Southwestern Medical Center at Dallas, 5323 Harry Hines Boulevard, Dallas, Texas 75390

<sup>3</sup>Department of Chemistry, Gulbarga University, Gulbarga 585 106, India

<sup>4</sup>Center of Excellence in Polymer Science, Karnatak University, Dharwad 580 003, India

Received 24 August 2004; accepted 27 September 2004

DOI 10.1002/app.21405

Published online in Wiley InterScience (www.interscience.wiley.com).

**ABSTRACT:** Novel nanocomposites of polyaniline dispersed with  $\gamma$ -Fe<sub>2</sub>O<sub>3</sub> nanoparticles were prepared by the in situ polymerization of aniline in the presence of ammonium peroxy sulfate as an oxidizing agent. Dielectric constants of the derived composites varied with the composition of  $\gamma$ -Fe<sub>2</sub>O<sub>3</sub> present in the matrix. A maximum dielectric constant of ~5500 was achieved when 10 mass %  $\gamma$ -Fe<sub>2</sub>O<sub>3</sub> nanoparticles were present. Nanocomposites were characterized by X-ray diffraction, Fourier transform infrared, scanning electron microscopy, and thermal analytical tech-

niques. Conductivity increased marginally by increasing the amount of  $\gamma$ -Fe<sub>2</sub>O<sub>3</sub> in the matrix. Dielectric constants increased 100–150 times compared to plain polyaniline matrix and were 20–40 times higher than that of  $\gamma$ -Fe<sub>2</sub>O<sub>3</sub> nanoparticles. © 2005 Wiley Periodicals, Inc. *J Appl Polym Sci* 97: 1868–1874, 2005

**Key words:** nanocomposites; polyaniline; dielectric properties; morphology; X-RD

## INTRODUCTION

Recently, polymeric nanocomposites (PNCs) containing metal oxides have attracted a great deal of interest from researchers because they frequently exhibit unexpected hybrid properties synergistically derived from both components.<sup>1,2</sup> The control and design of characteristic structural features on the nanometer scale impart them with tailored properties for diverse applications.<sup>3</sup> Researchers have attempted to enhance the desired properties of PNCs and, thus, to extend their utility by reinforcing them with nanoscale materials to derive improved properties compared to the more conventional particulate-filled microcomposites.<sup>4</sup> Thus, PNCs containing nanosized metal oxides have been extensively studied since they exhibit interesting properties with many applications such as quantum electronic devices, magnetic recording materials, sensors, capacitors, smart windows, toners in photocopying, conducting paints, and rechargeable

batteries.<sup>5–9</sup> However, due to poor mechanical properties of the many conducting polymers, they could not be processed easily.<sup>10–12</sup> By combining conducting polymers with metal oxide nanoparticles, one could produce PNCs, the properties of which can be tuned depending upon the composition of metal oxide in the polymer matrix. Nanocomposites of polyaniline (PANI) have been widely studied<sup>1,13–16</sup> in view of their unique electrical, dielectrical, optical, and optoelectrical properties in addition to their ease of preparation and excellent environmental stability.

Previously, we have reported<sup>17</sup> the nanocomposites of poly(methyl methacrylate) by dispersing with varying amounts of  $\gamma$ -Fe<sub>2</sub>O<sub>3</sub> nanoparticles, but these PNCs exhibited good thermal properties with low dielectric constants. Development of high dielectric constant PNCs has been a major challenge of integral capacitor technology.<sup>3,18</sup> High dielectric constant PNCs are being continuously explored by the electronics industries in response to the need for power-ground decoupling to secure integrity of high-speed signals with the reduced electromagnetic interference radiated noise.<sup>19,20</sup> Ceramic PNCs with dielectric constant up to 150 are of great interest as embedded capacitor materials because they combine the processability of polymers with the high dielectric constant of ceramics.<sup>21,22</sup> Some novel PNCs of epoxy and lead magnesium nio-

Correspondence to: T. M. Aminabhavi (aminabhavi@yahoo.com).

Contract grant sponsor: University Grants Commission, New Delhi, India.

This paper is CEPS Communication No. 55.

bate-lead titanate have been reported<sup>23</sup> with a dielectric constant value of 110. High dielectric constant ceramics employed to develop PNCs have been derived by the impregnation of niobates, titanates, zirconia ( $ZrO_2$ ), tantalum oxide ( $Ta_2O_5$ ), aluminum oxide ( $Al_2O_3$ ), etc. However, the interface adhesion between ceramics and polymer matrix is poor, especially when ceramic loading is high.<sup>24,25</sup>

Over the past decades, polyaniline (PANI) has emerged as one of the most promising organic conducting polymers, owing to its high polymerization yield and good chemical stability combined with moderate electrical conductivity and relatively low cost.<sup>26–28</sup> Nevertheless, some studies have indicated that PANI and PANI/polymer blends are capable of enhancing dielectric constant up to 104 in a partially crystalline PANI.<sup>14</sup> The present investigation reports a simple, yet elegant method to prepare PNCs using PANI that could exhibit very high dielectric constant. In this method, PANI was dispersed with 2, 5, and 10 mass %  $\gamma$ - $Fe_2O_3$  nanoparticles during in situ polymerization of aniline in the presence of ammonium persulfate,  $(NH_4)_2S_2O_8$ , as an oxidant. PNCs thus prepared were characterized by X-ray diffraction (X-RD), Fourier transform infrared (FTIR), scanning electron microscopy (SEM), and thermal analytical techniques. Conductivity increased marginally by increasing the amount of  $\gamma$ - $Fe_2O_3$  in the polymer matrix, but dielectric constants increased 100–150 times compared to the plain PANI and 20–40 times compared to  $\gamma$ - $Fe_2O_3$ . PNCs of this study can have potential applications as capacitors.

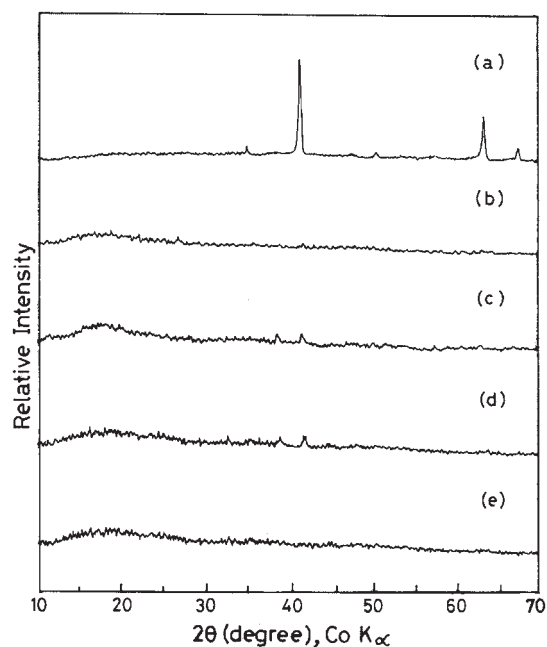


**Figure 1** X-RD tracings of (a) pure  $\gamma$ - $Fe_2O_3$ , (b) PANI-2, (c) PANI-5, (d) PANI-10, and (e) PANI-0 nanocomposites.

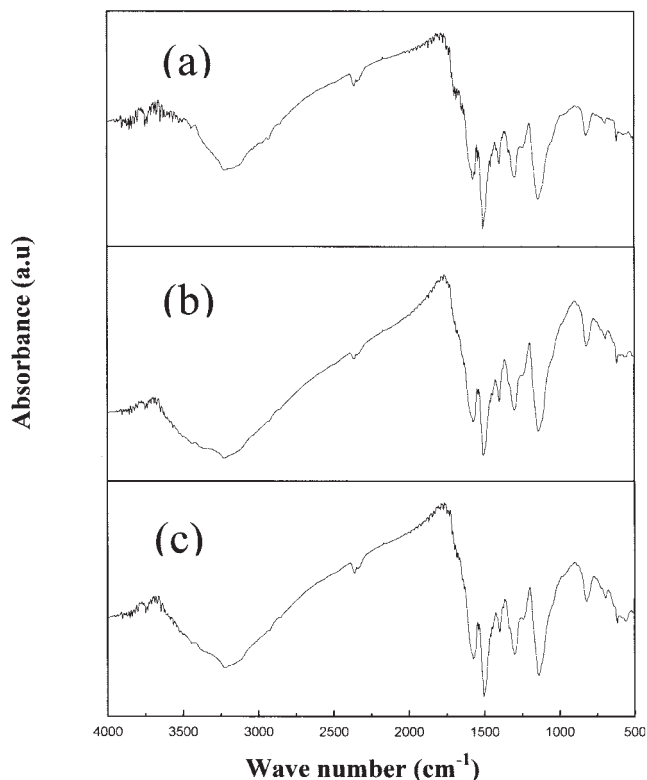


**Figure 2** FTIR tracings of (a) PANI-2, (b) PANI-5, and (c) PANI-10 nanocomposites.

## EXPERIMENTAL PROCEDURES

### Synthesis of $\gamma$ - $Fe_2O_3$ nanoparticles

$\gamma$ - $Fe_2O_3$  nanoparticles were prepared by the combustion route as described earlier.<sup>29,30</sup> In brief, ferric acetylacetonate was mixed with polyethylene glycol (PEG-4000) in a mass ratio of 1 : 5 and ground to a fine powder in a mortar with a pestle. The resulting solid was taken in a crucible and heated in air. Initially, polyethylene glycol was melted, frothed, and finally ignited to form  $\gamma$ - $Fe_2O_3$ . Upon cooling to room temperature, no traces of carbon impurities were left in the final residue of  $\gamma$ - $Fe_2O_3$ .

### Preparation of $\gamma$ - $Fe_2O_3$ -PANI nanocomposites

In a typical procedure, 2 mL of aniline was dissolved in 100 mL of 1 M HCl cooled to 0°C. About 2.3 g of  $(NH_4)_2S_2O_8$  in 100 mL of 1 M HCl was added to the reaction mixture along with 2, 5, or 10 mass %  $\gamma$ - $Fe_2O_3$  nanoparticles. The mixture was stirred vigorously for 30 min and allowed to stand for 60 min. The resultant product was filtered, washed thoroughly with water, and dried at 40°C until constant weight. The solution was made basic by adding ammonia until the change

in color was from green to blue and kept overnight with stirring, filtered, and dried. The PNCs thus obtained were designated PANI-0 (for plain PANI), PANI-2, PANI-5, and PANI-10 for 2, 5, and 10 mass % containing  $\gamma$ -Fe<sub>2</sub>O<sub>3</sub> nanoparticles, respectively.

### Characterization of PNCs

The powder X-RD patterns were recorded on a Jeol JDX-8P diffractometer using CoK<sub>α</sub> radiation ( $\lambda = 1.7901 \text{ \AA}$ ) at 30 kV. FTIR spectra were recorded on a Perkin-Elmer (Model No. 1000) spectrophotometer. Thermogravimetric analysis (TGA), differential thermal analysis (DTA), and differential scanning calorimetry (DSC) experiments were performed using Perkin-Elmer instruments. TGA and DTA data were obtained at a heating rate of 10°C/min under a static air atmosphere, while DSC experiments were carried out under a nitrogen atmosphere. SEM were taken on a Leica instrument (Model No. 440, Cambridge, UK). Dielectric measurements were taken on a HP-4192A impedance analyzer. Conductivity data were collected using a multimeter on pressed 1-cm pellets.

## RESULTS AND DISCUSSION

### X-ray diffraction

The X-ray diffraction patterns of plain  $\gamma$ -Fe<sub>2</sub>O<sub>3</sub> nanoparticles, nanocomposites of PANI with varying amounts of  $\gamma$ -Fe<sub>2</sub>O<sub>3</sub>, i.e., PANI-2, PANI-5, and PANI-10, and plain PANI are compared in Figure 1a, b, c, d, and e, respectively. A sharp peak observed for  $\gamma$ -Fe<sub>2</sub>O<sub>3</sub> particles is due to its highly crystalline nature. However, after the addition of  $\gamma$ -Fe<sub>2</sub>O<sub>3</sub> nanoparticles into PANI during polymerization, high-intensity peaks were masked due to the overwhelming amorphous nature of PANI, thereby masking the sharp peaks observed due to the crystalline nature of  $\gamma$ -Fe<sub>2</sub>O<sub>3</sub> nanoparticles. This also confirms the uniform molecular level dispersion of  $\gamma$ -Fe<sub>2</sub>O<sub>3</sub> in PANI, which is responsible for a decrease crystallinity of  $\gamma$ -Fe<sub>2</sub>O<sub>3</sub> particles upon dispersion into the PANI matrix.

### FTIR studies

FTIR studies were carried out to confirm the possible chemical interactions between  $\gamma$ -Fe<sub>2</sub>O<sub>3</sub> and PANI. As can be seen in Figure 2a–c, FTIR spectra of PANI-2, PANI-5, and PANI-10 are nearly identical, indicating no chemical interactions. The characteristic peaks observed for plain PANI<sup>31</sup> are identical to those of PNCs,

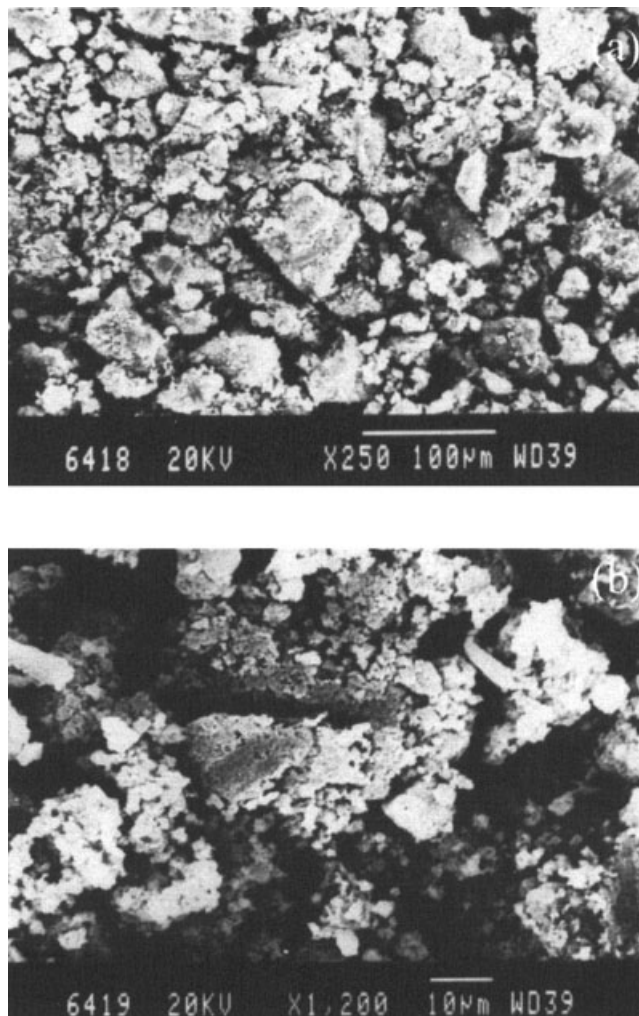


**Figure 3** SEM micrographs of (a) low-resolution and (b) high-resolution PANI-2 nanocomposites.

further confirming no chemical interactions between  $\gamma$ -Fe<sub>2</sub>O<sub>3</sub> and PANI.

### Morphological studies

The physical appearance of  $\gamma$ -Fe<sub>2</sub>O<sub>3</sub> loaded PANI was pale green to brownish-green depending upon the amount of  $\gamma$ -Fe<sub>2</sub>O<sub>3</sub> present. SEM micrographs of PANI-2 at low and high resolutions are displayed in Figure 3a and b, respectively. Particle size of PNCs as determined<sup>32</sup> by transmission electron microscopy varied between 25 and 100 nm for plain  $\gamma$ -Fe<sub>2</sub>O<sub>3</sub>. SEM micrographs of different PNCs did not show much variation and, hence, we have displayed typical SEM photographs of the PANI-2 matrix. It is worth mentioning here that when  $\gamma$ -Fe<sub>2</sub>O<sub>3</sub> nanoparticles were added to the reaction mixture, the polymerization reaction was much faster than

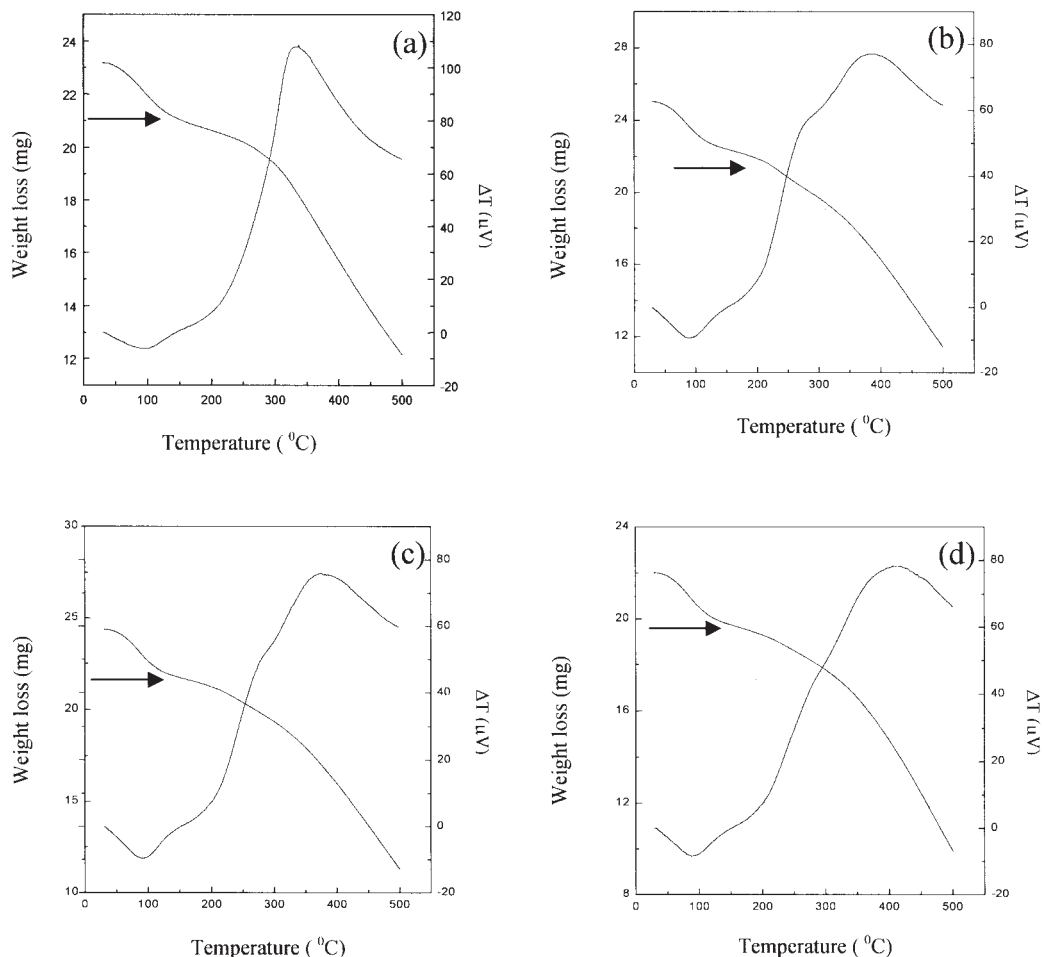


**Figure 4** TGA/DTA tracings of (a) PANI-0, (b) PANI-2, (c) PANI-5, and (d) PANI-10 nanocomposites.

the normal polymerization of aniline. This suggests that iron may act as a catalyst to foster the reaction. It may be noted that the time taken for complete polymerization in the presence of  $\gamma\text{-Fe}_2\text{O}_3$  nanoparticles is one-third the time required in the absence of iron oxide particles. Also, the color change observed during polymerization in the presence of  $\gamma\text{-Fe}_2\text{O}_3$  was dark green to brownish-green, while it was green to dark green when polymerization was carried out in the absence of  $\gamma\text{-Fe}_2\text{O}_3$ .

### Thermal analysis

TGA and DTA thermograms of the plain PANI and those of PANI-2, PANI-5, and PANI-10 nanocomposites are displayed in Figure 4a, b, c, and d, respectively. The TGA curve for plain PANI showed a rapid decomposition from about 100 until about 500°C. DTA curves showed endothermic peaks around 100°C, while exothermic peaks were observed around 370–400°C. The initial weight loss

observed in the TGA experiment and endothermic peaks could be attributed to the loss of moisture in PNCs. However, with increasing amounts of  $\gamma\text{-Fe}_2\text{O}_3$ , the decomposition temperature shifted to a higher value, indicating increased thermal stability of the PNCs. The DSC analysis presented in Figure 5a, b, and c, respectively, for PANI-2, PANI-5, and PANI-10 nanocomposites showed broad endothermic peaks around 300°C for PANI-2 and PANI-5, while for PANI-10 an exothermic peak was observed around 300°C with a sharp endothermic peak at about 250°C. Thermal analytical data indicated that thermal stability of PNCs decreased with increasing amount of  $\gamma\text{-Fe}_2\text{O}_3$ .

### Room temperature conductivity

Room temperature conductivity data presented in Figure 6 for the plain PANI as well as PANI-2, PANI-5, and PANI-10 samples showed only a marginal increase with increasing amounts of  $\gamma\text{-Fe}_2\text{O}_3$ . This might

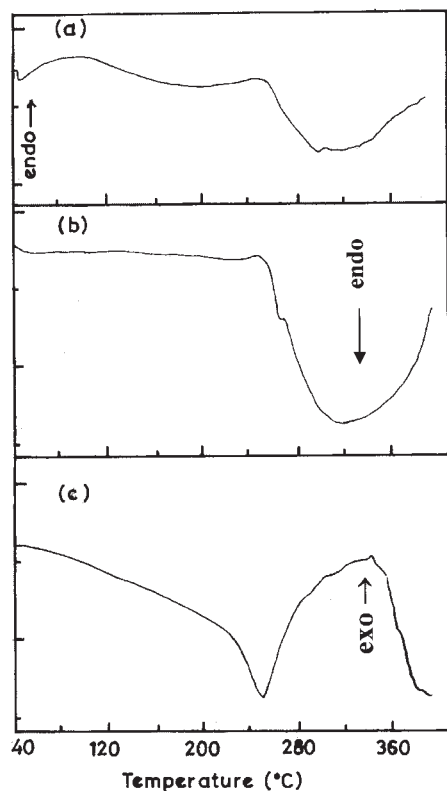


Figure 5 DSC tracings of (a) PANI-2, (b) PANI-5, and (c) PANI-10 nanocomposites.

be due to the ferromagnetic nature of  $\gamma$ -Fe<sub>2</sub>O<sub>3</sub>, which might cause an internal magnetic field, thereby increasing the conductivity.<sup>33,34</sup>

### Dielectric constant

To understand the dielectric behavior of PNCs developed in this study, we have investigated the variation of dielectric constant,  $\epsilon$ , and dielectric loss,  $\tan \delta$ , with frequency. Figure 7a shows the variation of  $\epsilon$  with frequency (ranging from 10<sup>2</sup> to 10<sup>7</sup> kHz). Plain PANI showed a steep decrease from its initial dielectric constant of 18 at 10<sup>2</sup> Hz to 5 at 10<sup>4</sup> Hz and thereafter it remained constant. The decrease in  $\epsilon$  was quite dramatic in the frequency range from  $2.5 \times 10^2$  to 10<sup>3</sup> Hz and thereafter the decrease in  $\epsilon$  was slow.  $\tan \delta$  also had a similar trend. Initially,  $\tan \delta = 8$ , which was changed to 0 at 10<sup>7</sup> Hz. Such values of  $\epsilon$  and  $\tan \delta$  are in general agreement with the nonconducting type PANI samples.

As shown in Figure 7b, dielectric constants decreased sharply from about 3500 at 10<sup>2</sup> Hz to 200 at 10<sup>3</sup> Hz and afterward remained almost constant. The  $\tan \delta$  values showed an initial value of 3 at 10<sup>2</sup> Hz and remained constant at  $2.8 \times 10^3$  Hz; thereafter the decrease in  $\tan \delta$  was slow, reaching 0 at 10<sup>7</sup> Hz. Figure

7c and d exhibits almost similar trends. We could observe a dramatic increase in  $\epsilon$  from  $\sim 35$  for PANI-0 and  $\sim 200$  for pure  $\gamma$ -Fe<sub>2</sub>O<sub>3</sub> to  $\sim 3500$  for PANI-2,  $\sim 4000$  for PANI-5, and  $\sim 5500$  for PANI-10 samples. These values are 20–40 and 100–150 times higher than those observed for plain  $\gamma$ -Fe<sub>2</sub>O<sub>3</sub> and PANI-0, respectively. This type of very high increase in  $\epsilon$  could be attributed to high packing density of  $\gamma$ -Fe<sub>2</sub>O<sub>3</sub> nanoparticles in PANI.

A steep decrease in dielectric constant, close to that of plain  $\gamma$ -Fe<sub>2</sub>O<sub>3</sub>, suggests that polarization dielectric might have been lost and the polymer is in a higher reduced state due to the presence of hydrogen atoms. These hydrogen atoms could participate in the partial reduction of Fe<sup>3+</sup> ions in an octahedral position of  $\gamma$ -Fe<sub>2</sub>O<sub>3</sub> particles, thereby creating Fe<sup>2+</sup> and Fe<sup>3+</sup> ions. Thus, reduction of Fe<sup>3+</sup> ions might have increased at higher frequency, thereby producing the possible intermediate compositions<sup>33</sup> like Fe<sub>8</sub><sup>3+</sup>[Fe<sub>x</sub><sup>2+</sup> H<sub>4-2x</sub> Fe<sub>12</sub><sup>3+</sup>]O<sub>32</sub>. Such  $\gamma$ -Fe<sub>2</sub>O<sub>3</sub> particles having an intermediate composition would contain Fe<sup>2+</sup> ions, which would also contribute to a decrease in dielectric constant. It can be understood from the earlier study<sup>35</sup> that conductivity increased in the presence of Fe<sup>2+</sup> ions through a hopping mechanism, further suggesting that  $\gamma$ -Fe<sub>2</sub>O<sub>3</sub> nanoparticles might have undergone a change from pure vacancy ordered  $\gamma$ -Fe<sub>2</sub>O<sub>3</sub> to an intermediate form, Fe<sub>8</sub><sup>3+</sup>[Fe<sub>x</sub><sup>2+</sup> H<sub>4-2x</sub> Fe<sub>12</sub><sup>3+</sup>]O<sub>32</sub>.

### CONCLUSIONS

PNCs were prepared by incorporating different amounts of  $\gamma$ -Fe<sub>2</sub>O<sub>3</sub> nanoparticles into a PANI matrix. These materials exhibited high dielectric constants that increased with increasing amount of  $\gamma$ -Fe<sub>2</sub>O<sub>3</sub>. The X-RD data suggested a uniform dispersion of  $\gamma$ -Fe<sub>2</sub>O<sub>3</sub> in all matrices. The addition of

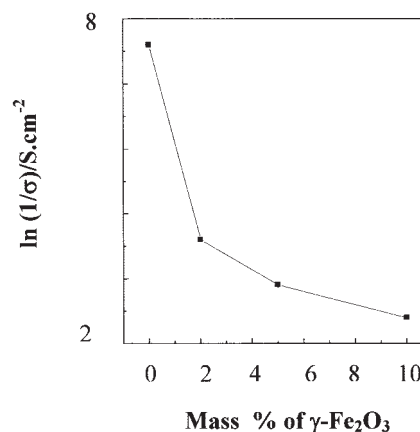
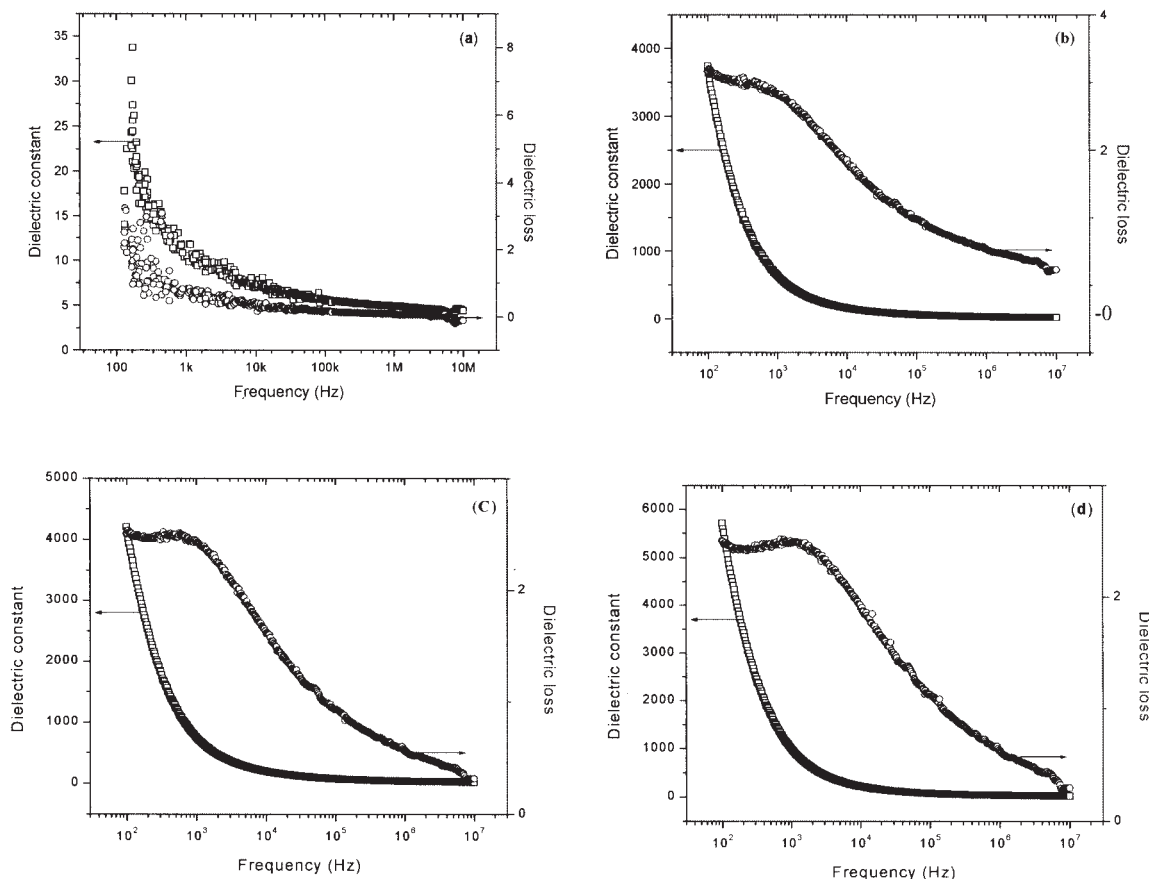


Figure 6 Conductivity versus mass %  $\gamma$ -Fe<sub>2</sub>O<sub>3</sub> loaded in nanocomposites.



**Figure 7** Dielectric constant and dielectric loss (room temperature) versus frequency for (a) PANI-0, (b) PANI-2, (c) PANI-5, and (d) PANI-10 nanocomposites.

$\gamma$ -Fe<sub>2</sub>O<sub>3</sub> into the PANI matrix increased conductivity only marginally, but the increase in dielectric constant with very low dielectric loss was quite considerable. The PNCs developed in this study may be useful as capacitors. However, more detailed studies on mechanical and magnetic susceptibility measurements of the PNCs are in progress and these will be reported in future articles.

This work represents collaborative efforts among Karnatak University, University of Texas at Dallas, UT Southwestern Medical Center at Dallas, and Gulbarga University. Results of this study represent part of the Ph.D. work undertaken by N. N. Mallikarjuna.

## References

- Maity, A.; Biswas, M. *J Appl Polym Sci* 2004, 94, 803.
- Alenxandre, M.; Dunois, P. *Mater Sci Eng* 2000, 28, 1.
- Holmes, C. C.; Vogt, T.; Shapiro, S. M.; Wakimoto, S.; Ramirez, A. P. *Science* 2001, 293, 673.
- Novak, B. M. *Adv Mater* 1993, 5, 422.
- Leu, C.-M.; Wu, Z.-W.; Wei, K.-H. *Chem Mater* 2002, 14, 3021.
- Wang, J.; Yang, J.; Xie, J.; Xu, N. *Adv Mater* 2002, 14, 963.
- Jiang, L.-H.; Leu, C.-M.; Wei, K.-H. *Adv Mater* 2002, 14, 426.
- Hughes, M.; Shaffer, M. S.; Renouf, P. A. C.; Singh, C.; Chen, G. Z.; Fray, D. J.; Windle, A. H. *Adv Mater* 2002, 14, 382.
- Vossmeier, T.; Guse, B.; Besnard, I.; Bauer, R. E.; Müllen, K.; Yasuda, A. *Adv Mater* 2002, 14, 238.
- Wang, Y.; Wang, X.; Li, J.; Mo, J.; Zhao, X.; Jing, X.; Wang, F. *Adv Mater* 2002, 13, 1582.
- MacDiarmid, A. G.; Epstein, A. *J Farad Discus* 1989, 88, 333.
- Roth, S.; Graupner, W. *Synth Metals* 1993, 57, 3623.
- Maeda, S.; Armes, S. P. *Chem Mater* 1995, 7, 171.
- Joo, J.; Long, S. M.; Pouget, J. P.; Oh, E. J.; MacDiarmid, A. G.; Epstein, A. *J Phys Rev B* 1998, 16, 9567.
- Li, Z. F.; Ruckenstein, E. *Langmuir* 2002, 18, 6956.
- Demets, G. J. F.; Anaissi, F. J.; Toma, H. E. *Electrochim Acta* 2000, 46, 547.
- Mallikarjuna, N. N.; Venkataraman, A.; Aminabhavi, T. M. *J Appl Polym Sci* 2004, 94, 2551.
- Sugii, N.; Yamada, H.; Kagaya, O.; Yamasaki, M.; Sekine, K.; Yamashita, K.; Watanabe, M.; Murakami, S. *Appl Phys Lett* 1998, 72, 261.
- Popielarz, R.; Chiang, C. K.; Nozaki, R.; Obrzut, J. *Macromolecules* 2001, 34, 5910.
- Koul, S.; Chandra, R.; Dhawan, S. K. *Polymer* 2000, 41, 9305.
- Rao, Y.; Ogitani, S.; Kohl, P.; Wong, C. P. *J Appl Polym Sci* 2002, 83, 1084.
- Zhang, M.; Li, H. F.; Poh, M.; Xia, F.; Chang, Z.-Y.; Xu, H. S.; Huang, C. *Nature* 2002, 419, 284.
- Rao, Y.; Yue, J.; Wong, C. P. *Active Passive Elect Comp* 2002, 25, 123.

24. Wong, C. P.; Bollampally, R. S. *J Appl Polym Sci* 1999, 74, 3396.
25. Yang, T. C.-K.; Tsai, S. H.-Y.; Wang, S.-F.; Juan, C.-C. *Comp Sci Technol* 2002, 62, 655.
26. Nalwa, H. S., *Handbook of Organic Conductive Molecules and Polymers*, Vol. 2, Wiley, New York, 1997.
27. Jia, W.; Tchondakov, K.; Segal, E.; Joseph, R.; Narkis, M.; Siegmann, A. *Synth Metals* 2003, 132, 269.
28. Zhang, X.; Goux, W.; Manohar, S. K. *J Am Chem Soc* 2004, 126, 4502.
29. Mallikarjuna, N. N.; Govindaraj, B.; Lagashetty, A.; Venkataraman, A. *Thermal Anal Calor* 2002, 69, 901.
30. Mallikarjuna, N. N.; Venkataraman, A. *Talanta* 2003, 60, 139.
31. Stejskal, J.; Sapurina, I.; Trchova, M.; Prokes, J.; Krivka, I.; Tobolkova, E. *Macromolecules* 1998, 31, 2218.
32. Laska, J.; Widlarz, J. *Synth Metals* 2003, 261, 135.
33. Chwang, C. P.; Wang, C. L.; Kuo, Y. M.; Lee, S. N.; Chao, A.; Chao, D. Y. *Polym Adv Technol* 2002, 13, 285.
34. Haba, H.; Segal, E.; Narkis, M.; Titelman, G. I.; Siegmann, A. *Synth Metals* 2000, 110, 189.
35. Bae, W. J.; Jo, W. H.; Park, Y. H. *Synth Metals* 2003, 132, 239.
36. Jia, W.; Segal, E.; Kornemandel, D.; Lambot, Y.; Narkis, M.; Siegmann, A. *Synth Metals* 2002, 128, 115.